

# Effects of finite poloidal gyroradius, shaping, and collisions on the zonal flow residual<sup>a)</sup>

Yong Xiao<sup>b)</sup> and Peter J. Catto

*Plasma Science and Fusion Center, Massachusetts Institute of Technology, Cambridge, Massachusetts 02139*

William Dorland

*Department of Physics, University of Maryland, College Park, Maryland 20742*

(Received 4 November 2006; accepted 24 February 2007; published online 11 May 2007)

Zonal flow helps reduce and regulate the turbulent transport level in tokamaks. Rosenbluth and Hinton have shown that zonal flow damps to a nonvanishing residual level in collisionless [M. Rosenbluth and F. Hinton, *Phys. Rev. Lett.* **80**, 724 (1998)] and collisional [F. Hinton and M. Rosenbluth, *Plasma Phys. Control. Fusion* **41**, A653 (1999)] banana regime plasmas. Recent zonal flow advances are summarized including the evaluation of the effects on the zonal flow residual by plasma cross-section shaping, shorter wavelengths including those less than an electron gyroradius, and arbitrary ion collisionality relative to the zonal low frequency. In addition to giving a brief summary of these new developments, the analytic results are compared with GS2 numerical simulations [M. Kotschenreuther, G. Rewoldt, and W. Tang, *Comput. Phys. Commun.* **88**, 128 (1991)] to demonstrate their value as benchmarks for turbulence codes. © 2007 American Institute of Physics. [DOI: [10.1063/1.2718519](https://doi.org/10.1063/1.2718519)]

## I. INTRODUCTION

Recent discoveries in plasma turbulence show that zonal flow is an important mechanism for suppressing ion temperature gradient (ITG)<sup>1-3</sup> and trapped electron mode (TEM)<sup>4,5</sup> turbulence. As a result, it is important to understand the damping mechanisms that act on zonal flow. The original Rosenbluth-Hinton (R-H) study showed that zonal flow is modified by the collisionless neoclassical polarization, with a significant residual flow surviving due to the smallness of this polarization.<sup>6</sup> Later, Hinton-Rosenbluth (H-R) found that in the large radial wavelength limit collisional effects significantly reduce the residual zonal flow to a level much smaller<sup>7</sup> than the collisionless kinetic theory predicts.<sup>6</sup> Both of these analytical studies are based on a large aspect ratio circular flux surface tokamak model.

Three aspects of these pioneering studies on the linear damping of zonal flow have been extended recently. First, in the large radial wavelength limit, the original R-H collisionless residual zonal flow calculation<sup>6</sup> has been generalized to more realistic flux surface shapes that allow elongation, triangularity, and Shafranov shift to be retained in the equilibrium model.<sup>8</sup> Second, the original R-H collisionless calculation has been extended to cover arbitrary radial wavelength zonal flow,<sup>9</sup> including, in particular, shorter wavelength effects of interest for ITG and TEM modes and the still shorter wavelengths associated with electron temperature gradient (ETG) turbulence. Finally, a new method has been developed to study collisional zonal flow damping.<sup>10</sup> This new analytical approach is valid for arbitrary collisionality and long wavelengths, and is therefore a useful extension of the original H-R collisional work.<sup>11,12</sup>

These new developments in the R-H and H-R zonal flow studies provide not only new insights on the physics of residual zonal flow, but also new opportunities to crosscheck numerical simulations. Some of these checks for the well-known continuum turbulence code GS2 are presented here.<sup>13</sup> Previously, the GS2 code had successfully benchmarked the well-known R-H collisionless residual zonal flow calculation.<sup>14</sup> This code also discovered the increase in the residual zonal flow at short radial wavelength driven by ETG, ITG, and TEM turbulence.<sup>15</sup> Moreover, a prior GS2 study on shaping effects<sup>16</sup> gave results similar to the analytical theory of reference.<sup>8</sup> Therefore, it is desirable to make a more thorough and careful comparison between the new analytical developments<sup>8-10</sup> and the numerical simulations using the GS2 code under common circumstances and parameters.

This paper is organized as follows. Sections II and III review the linear gyrokinetics of zonal flow and the recent extensions of the R-H and H-R zonal flow models. In Sec. IV, we briefly summarize the new analytical results for plasma shaping effects and compare them to the GS2 numerical simulations. Section V briefly reviews the recent analytical calculation of collisionless residual zonal flow for the arbitrary radial wavelength and compares it to the GS2 simulation result. In Sec. VI, we compare the collisional damping of zonal flow from the GS2 code to the recent analytical result. Finally, Sec. VII provides a brief discussion summarizing the newly discovered results including the comparisons discussed in the preceding sections.

## II. LINEAR GYROKINETICS DRIVEN BY ZONAL FLOW

The linearized gyrokinetic equation can be employed to study the linear response of the plasma to an axisymmetric zonal flow potential caused by turbulence.<sup>6</sup> The distribution function is assumed to be composed of two parts: the unper-

<sup>a)</sup>Paper GII 6, *Bull. Am. Phys. Soc.* **51**, 99 (2006).

<sup>b)</sup>Invited speaker. Present address: Physics and Astronomy, University of California, Irvine, CA 92697.

turbed and the perturbed. The unperturbed part is assumed to be a radially slowly varying Maxwellian  $F_0$ . The perturbed part is driven by the zonal flow potential and has the form  $f = -e\phi/TF_0 + g$ , where the adiabatic response has been separated out for convenience. Here we assume that all the perturbed quantities take an eikonal form  $\phi = \sum_k \phi_k e^{iS}$  with the eikonal  $S = S(\psi)$  and the radial wave vector  $\mathbf{k}_\perp = \nabla S$ . Then in the Fourier space, the guiding center distribution  $g_k$  satisfies the following gyrokinetic equation:<sup>6,17,18</sup>

$$\frac{\partial g_k}{\partial t} + (v_\parallel \mathbf{b} \cdot \nabla + i\omega_D)g_k - C\{g_k\} = \frac{e}{T} F_0 J_0 \frac{\partial \phi_k}{\partial t}, \quad (1)$$

where  $C$  is the gyroaveraged collision operator,  $J_0$  is the zeroth-order Bessel function,  $J_0 = J_0(k_\perp v_\perp / \Omega)$ , and  $\omega_D = \mathbf{k}_\perp \cdot \mathbf{v}_d = v_\parallel \mathbf{b} \cdot \nabla Q$  with  $Q = IS'v_\parallel / \Omega$  coming from the magnetic drift  $\mathbf{v}_d = \mathbf{b} / \Omega \times (\mu \nabla B + v_\parallel^2 \mathbf{b} \cdot \nabla \mathbf{b})$  since  $\mathbf{v}_d \cdot \nabla \psi = v_\parallel \mathbf{b} \cdot \nabla (Iv_\parallel / \Omega)$ . Notice  $Q \sim k_\perp \rho_p$ , where  $\rho_p$  is the poloidal gyroradius. The independent velocity variables used in the preceding equation are kinetic energy  $E = v^2/2$  and magnetic moment  $\mu = v_\perp^2/2B$ . For simplicity, hereafter we assume hydrogenic ions in the plasma.

Since the zonal flow frequency  $\omega$  considered here is far below the transit frequency of thermal particles  $\omega_t = v_T/qR_0$ , the equation can be solved perturbatively by expanding in  $\omega/\omega_t \ll 1$  (Ref. 6) by letting  $g_k = g_k^0 + g_k^1 + \dots$ . The leading-order equation in this expansion gives

$$v_\parallel \mathbf{b} \cdot \nabla g_k^0 + iv_\parallel g_k^0 \mathbf{b} \cdot \nabla Q = 0, \quad (2)$$

whose solution has the form  $g_k^0 = h_k e^{-iQ}$  with  $\mathbf{b} \cdot \nabla h_k = 0$ . Then next-order equation gives

$$v_\parallel \mathbf{b} \cdot \nabla g_k^1 + iv_\parallel g_k^1 \mathbf{b} \cdot \nabla Q = -\frac{\partial g_k^0}{\partial t} + C\{g_k^0\}_\varphi + \frac{e}{T} F_0 J_0 \frac{\partial \phi_k}{\partial t}. \quad (3)$$

The transit average of the product of this equation times  $e^{iQ}$  gives

$$\frac{\partial h_k}{\partial t} - \overline{e^{iQ} C\{h_k e^{-iQ}\}} = \frac{e}{T} F_0 J_0 \overline{e^{iQ}} \frac{\partial \phi_k}{\partial t}, \quad (4)$$

where the transit average is defined as  $\bar{A} = \oint d\tau A / \oint d\tau$ , with  $d\tau = d\theta / (v_\parallel \mathbf{b} \cdot \nabla \theta)$ . For trapped particles, this average is over a full bounce; while for passing particles it is over one complete poloidal circuit. Specifically, for a large aspect ratio circular cross-section tokamak,  $d\tau \cong qR_0 d\theta / v_\parallel$ , where  $q$  is the safety factor. In this case the transit average becomes

$$\bar{A} = \frac{\oint \frac{d\theta}{v_\parallel} A}{\oint \frac{d\theta}{v_\parallel}}. \quad (5)$$

When calculating the perturbed particle density in a flux surface, we utilize

$$\tilde{n}_k = \left\langle \int d^3 v J_0 h_k e^{-iQ} \right\rangle - \frac{e \phi_k}{T} n_0, \quad (6)$$

where  $\langle \rangle$  represents the flux surface average  $\langle A \rangle = \oint dl / BA / \oint dl / B$ .

If the time scale of interest is much shorter than a typical collision time, the plasma can be treated as collisionless; otherwise collisions must be retained. For the collisionless case, the solution to the transit average kinetic equation, Eq. (4), is straightforward,

$$h_k = \frac{e \phi_k}{T} F_0 \overline{J_0 e^{iQ}}. \quad (7)$$

Hence, the perturbed particle density in Eq. (6) can be expressed as

$$\tilde{n}_k = \frac{e \phi_k}{T} n_0 \left( \frac{1}{n_0} \left\langle \int d^3 v J_0 e^{-iQ} \overline{J_0 e^{iQ}} F_0 \right\rangle - 1 \right), \quad (8)$$

where the classical gyromotion effect (finite Larmor radius) on polarization is retained in  $J_0$ , and the effect of magnetic drift (finite poloidal gyroradius) is retained in  $e^{iQ}$ .

For the collisional case, the transit average kinetic equation (4) can only be solved for large radial wavelength zonal flow where  $k_\perp \rho_{pi} \ll 1$ . The ITG and TEM mode driven zonal flows fall into this category. Expanding Eqs. (4) and (6) to order  $Q^2$  (Refs. 7 and 10), we find

$$\tilde{n}_k = -\frac{e \phi_k}{T} n_0 \left[ \langle k_\perp^2 \rho^2 \rangle + \frac{1}{n_0} \left\langle \int d^3 v F_0 \left( Q^2 + \frac{iQ Th_k^{(1)}}{e \phi_k F_0} \right) \right\rangle \right], \quad (9)$$

where the distribution function  $h_k^{(1)}$  satisfies

$$\frac{\partial h_k^{(1)}}{\partial t} - \overline{C\{h_k^{(1)}\}} = i \overline{Q} \frac{e}{T} F_0 \frac{\partial \phi_k}{\partial t}. \quad (10)$$

We define the gyroradius as  $\rho = \sqrt{T/m}/\Omega$  with the gyrofrequency  $\Omega = eB/mc$ .

Next, we will review the Rosenbluth-Hinton zonal flow physics and its relationship to the current linear density calculation.

### III. GENERALIZED ROSENBLUTH-HINTON ZONAL FLOW PHYSICS

Quasineutrality of the plasma requires that the linear perturbed charge density be compensated by the nonlinear turbulent charge source, i.e.,  $e \tilde{n}_k^{(i)} - e \tilde{n}_k^{(e)} = -\rho_k^{NL}$ . In the Rosenbluth-Hinton zonal flow model, turbulence produces a constant initial charge source within a time that is much shorter than one transit time but much larger than one gyroperiod. Therefore, drift and collisional effects can be ignored ( $Q=0=C$ ) on such short time scales and the initial zonal flow potential is given by

$$\left[ \tau \left( \frac{1}{n_0} \left\langle \int d^3 v \overline{J_{0i}^2} F_{0i} \right\rangle - 1 \right) + \left( \frac{1}{n_0} \left\langle \int d^3 v \overline{J_{0e}^2} F_{0e} \right\rangle - 1 \right) \right] \frac{n_0 e^2}{T_e} \phi_k(t=0) = -\rho_k^{NL}(0), \quad (11)$$

according to Eq. (8) and quasineutrality, where  $\tau = T_e/T_i$ . For the long-wavelength ITG and/or TEM zonal flow cases,  $k_{\perp}\rho_{pi} \ll 1$ , this equation simplifies considerably to become

$$\frac{n_0 e^2}{T_i} \phi_k(t=0) \langle k_{\perp}^2 \rho_i^2 \rangle = -\rho_k^{NL}(0). \quad (12)$$

After several transit periods, drift effects become important. In the collisionless limit, the long-time zonal flow is then given by

$$\frac{\phi_k(t=\infty)}{\phi_k(t=0)} = \frac{\tau \left( \frac{1}{n_0} \left\langle \int d^3 v J_{0i}^2 F_{0i} \right\rangle - 1 \right) + \left( \frac{1}{n_0} \left\langle \int d^3 v J_{0e}^2 F_{0e} \right\rangle - 1 \right)}{\tau \left( \frac{1}{n_0} \left\langle \int d^3 v J_{0i} e^{-iQ_i} \overline{J_{0i} e^{iQ_i} F_{0i}} \right\rangle - 1 \right) + \left( \frac{1}{n_0} \left\langle \int d^3 v J_{0e} e^{-iQ_e} \overline{J_{0e} e^{iQ_e} F_{0e}} \right\rangle - 1 \right)}. \quad (14)$$

In the long-wavelength limit  $k_{\perp}\rho_{pi} \ll 1$ , the collisionless zonal flow residual reduces to

$$\frac{\phi_k(t=\infty)}{\phi_k(t=0)} = \frac{\langle k_{\perp}^2 \rho_i^2 \rangle}{\langle k_{\perp}^2 \rho_i^2 \rangle + \frac{1}{n_0} \left\langle \int d^3 v F_{0i} (Q_i^2 - \overline{Q_i^2}) \right\rangle}. \quad (15)$$

Collisional effects become significant when the time scales of interest are comparable to a typical collision time. At present, the collisional case is only tractable for the large wavelength zonal flow. In this case, the bounce average drift kinetic equation, Eq. (10), must be solved to evaluate the linearized particle density in Eq. (9). It is generally more convenient to solve Eq. (10) in the frequency domain,

$$h_k^{(1)}(p) - \frac{1}{p} \overline{C\{h_k^{(1)}(p)\}} = i \overline{Q} \frac{e}{T} F_0 \phi_k(p), \quad (16)$$

which comes from the Laplace transform of Eq. (10). The Laplace transforms of  $\phi_k$  and  $h_k^{(1)}$  are defined by  $\phi_k(p) = \int_0^{\infty} dt e^{-pt} \phi_k(t)$  and  $h_k^{(1)}(p) = \int_0^{\infty} dt e^{-pt} h_k^{(1)}(t)$ , where  $p$  is the frequency variable. In the frequency domain, the quasineutrality condition becomes

$$\frac{n_0 e^2}{T_i} \phi_k(p) \left[ \langle k_{\perp}^2 \rho_i^2 \rangle + \frac{1}{n_0} \left\langle \int d^3 v F_{0i} \left( Q_i^2 + \frac{i Q_i T_i h_k^{(1)}(p)}{e \phi_k F_0} \right) \right\rangle \right] = \frac{\rho_k^{NL}(0)}{p}, \quad (17)$$

where the distribution  $h_k^{(1)}(p)$  satisfies Eq. (16) for ions. The perturbed electron charge density is normally ignored because it is a mass ratio smaller than the ion part for ITG and TEM zonal flows. This equation, together with Eq. (12), gives the frequency response of the zonal flow to be

$$\left[ \tau \left( \frac{1}{n_0} \left\langle \int d^3 v J_{0i} e^{-iQ_i} \overline{J_{0i} e^{iQ_i} F_{0i}} \right\rangle - 1 \right) + \left( \frac{1}{n_0} \left\langle \int d^3 v J_{0e} e^{-iQ_e} \overline{J_{0e} e^{iQ_e} F_{0e}} \right\rangle - 1 \right) \right] \times \frac{n_0 e^2}{T_e} \phi_k(t=\infty) = -\rho_k^{NL}(0). \quad (13)$$

Therefore, the zonal flow residual that is customarily defined to be  $\phi_k(t=\infty)/\phi_k(t=0)$  has the form,

$$\frac{\phi_k(p)}{\phi_k(t=0)} = \frac{\langle k_{\perp}^2 \rho_i^2 \rangle / p}{\langle k_{\perp}^2 \rho_i^2 \rangle + \frac{1}{n_0} \left\langle \int d^3 v F_{0i} \left( Q_i^2 + \frac{i Q_i T_i h_k^{(1)}(p)}{e \phi_k F_0} \right) \right\rangle}. \quad (18)$$

The time evolution of zonal flow is then given by the following inverse Laplace transform:

$$\frac{\phi_k(t)}{\phi_k(t=0)} = \frac{1}{2\pi i} \int dp e^{pt} \frac{\phi_k(p)}{\phi_k(t=0)}. \quad (19)$$

Therefore, the long-time behavior of zonal flow or the zonal flow residual is determined by the zero-frequency response of Eq. (18), and the damping rate of the zonal flow is determined by the zeroes of the term  $\langle k_{\perp}^2 \rho_i^2 \rangle + 1/n_0 \langle \int d^3 v F_{0i} (Q_i^2 + i Q_i T_i h_k^{(1)}(p)/e \phi_k F_0) \rangle$ .

The following sections will briefly discuss three different recent developments that extend the R-H and H-R zonal flow calculations, and briefly present comparisons to the corresponding GS2 simulations.

#### IV. PLASMA SHAPING EFFECTS ON ZONAL FLOW RESIDUAL

The shaping factors for magnetic flux surfaces, such as elongation, triangularity, and Shafranov shift, are important ingredients in suppressing turbulent transport in tokamaks.<sup>19</sup> Recent numerical<sup>16</sup> and analytical<sup>8</sup> studies show that shaping also acts on the collisionless residual zonal flow level. Although these two approaches are based on different equilibrium models, they show similar dependences on plasma shaping. Here we provide a more careful comparison between the analytical formula and GS2 numerical simulation.

The analytical approach applies a global equilibrium,<sup>20</sup> whose flux surface in the large aspect ratio limit can be simplified to<sup>8</sup>

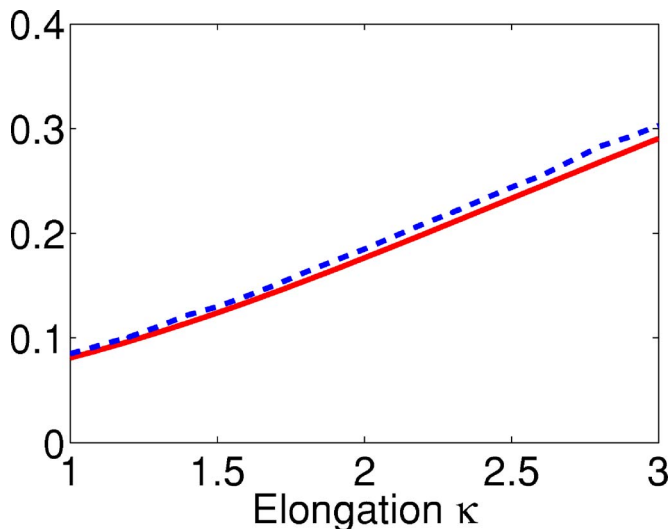


FIG. 1. Zonal flow residual dependence on elongation  $\kappa$ , for  $q=1.4$ ,  $\varepsilon=0.1$ ,  $\delta=0$ ,  $\Delta=0$ . The solid line is the analytical result and the dashed line is the GS2 simulation result.

$$R = R_0(1 + \varepsilon \cos \theta - \Delta - \delta \varepsilon \sin^2 \theta), \quad (20)$$

$$Z = R_0 \kappa \varepsilon \sin \theta, \quad (21)$$

while keeping the important shapings, such as elongation  $\kappa$ , triangularity  $\delta$ , and Shafranov shift  $\Delta$ , in the model. This model equilibrium has  $B_p = |\nabla \psi|/R$  with  $\psi = 4\varepsilon^2 \psi_0 = R_0 \kappa \varepsilon^2 / 2q$  and

$$|\nabla r| = \frac{\sqrt{\kappa^2 \cos^2 \theta + \sin^2 \theta + 4\delta \sin^2 \theta \cos \theta + 4\delta^2 \sin^2 \theta \cos^2 \theta}}{(1 - 2(\Delta/\varepsilon) \cos \theta)},$$

with  $q$  the safety factor. In this model, the triangularity  $\delta$  is assumed to be  $\propto \varepsilon$  and Shafranov shift  $\Delta \propto \varepsilon^2$ , while the elongation  $\kappa$  is a constant. To lowest order,  $B_p = I\varepsilon/R_0 q \sqrt{\kappa^2 \cos^2 \theta + \sin^2 \theta}$ . For a large aspect ratio tokamak, an  $\varepsilon$  expansion can be applied to calculate the zonal flow residual in Eq. (16) to obtain

$$\frac{\phi_k(t=\infty)}{\phi_k(t=0)} = \frac{1}{1 + Sq^2/\sqrt{\varepsilon}}, \quad (22)$$

with the shaping function  $S$  given by

$$S = \frac{1}{1 + \kappa^2} \left( 3.27 + \sqrt{\varepsilon} + 0.722\varepsilon - 1.443\delta - 2.945\frac{\Delta}{\varepsilon} + \frac{0.692\kappa^2 - 0.722}{q^2} \varepsilon \right). \quad (23)$$

This analytical result can be compared to GS2 simulations, as shown in Figs. 1 and 2. In Fig. 1, the elongation dependence of the zonal flow residual is compared to GS2 simulation, showing very good agreement. In Fig. 2,  $\kappa=1.8$ , and the triangularity dependence of the zonal flow residual is compared to GS2 simulation. The slope of these two curves are the same, telling us that the coefficient of the dependence of  $\delta$  in the shaping function is the same. The small differences between the GS2 results and Eq. (21) are due to the differing  $\varepsilon$  dependence of the global analytical and the local

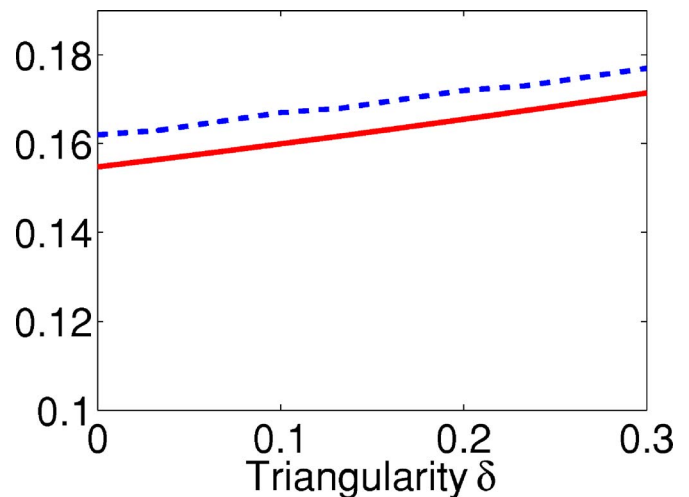


FIG. 2. Zonal flow residual dependence on triangularity  $\delta$ , for  $q=1.4$ ,  $\varepsilon=0.1$ ,  $\kappa=1.8$ ,  $\Delta=0$ . The solid line is the analytical result and the dashed line is the GS2 simulation result.

GS2 numerical equilibrium models in higher order. Shafranov shift comparisons cannot be meaningfully performed because the global model used to obtain the analytic results assumes  $\Delta$  is of order  $\varepsilon^2$ , while the local model in GS2 assumes  $\Delta$  is of order  $\varepsilon$  (as in the Miller *et al.* model<sup>19</sup>) and does not treat order  $\varepsilon^2$  corrections in the same way as the global model.

We see that the leading-order effect of shaping is due to elongation, which comes from the increase of the poloidal field  $B_p$  with elongation  $\kappa$  when keeping the safety factor  $q$  fixed. The triangularity effect is due to the change of the trapped-passing boundary location and therefore the change in the ratio between the trapped and passing particles.

## V. SHORT WAVELENGTH EFFECTS ON ZONAL FLOW RESIDUAL

In the preceding section, the plasma shaping effects on the collisionless residual zonal flow were considered. In this section and the following one, a large aspect ratio circular tokamak is considered (with the elongation  $\kappa=1$ , triangularity  $\delta=0$ , and Shafranov shift  $\Delta=0$ ).

The pioneering calculation of R-H (Ref. 6) focused on ITG mode driven zonal flow in the large wavelength limit satisfying  $k_{\perp} \rho_{pi} \ll 1$ . However, both experiments<sup>21</sup> and simulations<sup>22</sup> show that these zonal flows can have radial wavelength comparable to the ion poloidal gyroradius. Moreover, sources of anomalous transport, such as the trapped electron mode<sup>4,5</sup> and electron temperature gradient mode,<sup>11,12</sup> can also drive zonal flows at shorter radial wavelengths than the ion gyroradius. Indeed, for ETG turbulence, wavelengths as short as the electron gyroradius must be considered. Such short wavelength zonal flows were not considered by the original R-H calculation. Here we briefly summarize a recent study of the short wavelength effects collisionless zonal flow damping.<sup>9</sup>

Before doing so we recall that when the radial wavelength is much larger than the ion poloidal gyroradius,

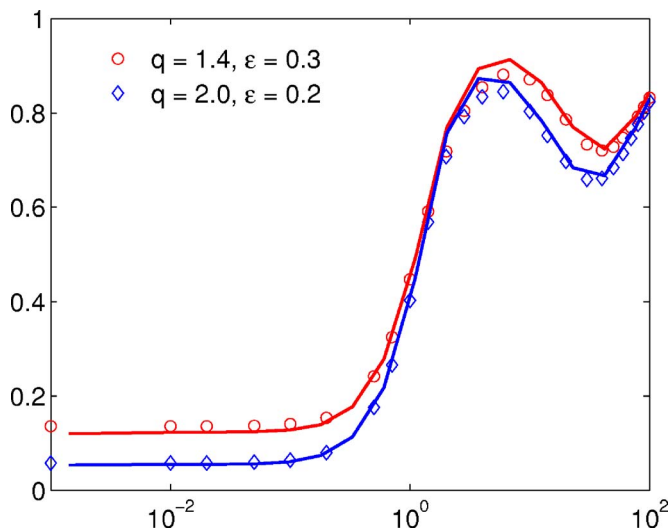


FIG. 3. The zonal flow residual  $\phi_k(t=\infty)/\phi_k(t=0)$  varies with normalized radial wavelength  $k_\perp \rho_i$ . The discrete shapes are from GS2 simulation. The solid lines are based on Eq. (14) as taken from Ref. 9.

$k_\perp \rho_{pi} \ll 1$ , Eq. (15) leads to the R-H value of the zonal flow residual,

$$\frac{\phi_k(t=\infty)}{\phi_k(t=0)} = \frac{1}{1 + \frac{q^2}{\epsilon^2} \Theta}, \quad (24)$$

with  $\Theta = 1.635\epsilon^{3/2} + 0.500\epsilon^2 + 0.360\epsilon^{5/2}$  and no dependence on the radial wave number  $k_\perp$ . The higher-order terms retained in the preceding expression make the result more accurate for the finite size  $\epsilon$  values than the original R-H coefficient  $1.6\epsilon^{3/2}$  (Ref. 9).

When the radial wavelength becomes close to the ion poloidal gyroradius, the finite poloidal gyroradius effect tries to increase the residual zonal flow level,

$$\frac{\phi_k(t=\infty)}{\phi_k(t=0)} = \frac{1}{1 + \frac{q^2}{\epsilon^2} (\Theta - 2.44\epsilon^{5/2} k_\perp^2 \rho_{pi}^2)}. \quad (25)$$

This result is valid for  $k_\perp \rho_i \ll 1$  and  $k_\perp \rho_{pi}$  approaching unity.<sup>9</sup>

As the radial wavelength gets even shorter, Eq. (14) needs to be numerically evaluated to obtain the collisionless zonal flow residual. When the radial wavelengths are small compared to an ion gyroradius, but comparable to or less than a poloidal electron gyroradius, electron polarization becomes important. The zonal flow residual first decreases with  $k_\perp$  due to electron neoclassical polarization. Then, the zonal flow residual recovers and increases due to finite electron poloidal gyroradius effects. Finally, as the radial wavelengths become much less than an electron gyroradius, the zonal flow residual ultimately approaches unity.

The preceding behavior was observed by Jenko *et al.* in GS2 simulations for ETG modes,<sup>15</sup> but for a slightly different driving source function. A careful comparison between the predictions of Eq. (14) and GS2 for the same source functions and parameters has now been performed to obtain the plots shown in Fig. 3. The agreement between these two

independent calculations is excellent and provides a useful benchmark of the zonal flow residual for arbitrary radial wavelengths.

Based on this figure, we expect ETG turbulence to saturate at a low level if short wavelength zonal flow is generated by the parasitic instabilities associated with ETG, ITG, and/or TEM modes. The high level of ETG turbulence sometimes observed in codes may indicate that the parasitic instabilities associated with ETG modes are not as effective in generating zonal flow as those associated with ITG and TEM modes.<sup>15,23</sup> Even though ITG and ETG modes are closely related to lowest order in linear theory (they are often referred to as isomorphic), the details of the zonal flows they ultimately generate are sensitive to the differences that show up in higher order and nonlinear behavior. For example, Candy and Waltz have found that the nonadiabatic behavior of the ions is important to retain,<sup>3</sup> and that the zonal flows generated are sensitive to whether one or both of the ITG and/or ETG modes are excited.<sup>24</sup> Moreover, Kim *et al.*<sup>25</sup> observe that some of the differing behavior may be due to the stronger collisional damping of the very short wavelength poloidal flows of interest for ETG modes.

## VI. COLLISIONAL ZONAL FLOW DAMPING FOR LARGE WAVELENGTH ZONAL FLOW

When the time scale of interest is on the order of the ion-ion collisional time  $\tau_{ii}$ , the collisional damping of zonal flow becomes important. The original H-R calculation<sup>7</sup> considers two asymptotic limits: the short-time or weak collision limit  $p\tau_{ii} \gg 1$ , and the long-time or strong collision limit  $p\tau_{ii} \ll 1$ , and ignores the need to conserve momentum in like particle collisions. To obtain an improved estimate of the decay rate it is desirable to obtain the frequency response of Eq. (18) for arbitrary values of  $p\tau_{ii}$ . A new method based on an eigenfunction expansion of the pitch angle scattering operator with a momentum conserving term retained has been developed to solve this problem.<sup>10</sup> It finds that in the large wavelength limit, Eq. (19) can be approximated by retaining an additional pole to find

$$\frac{\phi_k(t)}{\phi_k(t=0)} = \frac{\epsilon^2/q^2}{1 + \epsilon^2/q^2} \left[ 1 + \frac{1 - \Theta}{\Theta + \epsilon^2/q^2} e^{-(1+\epsilon^2/q^2)\Gamma/\Theta + \epsilon^2/q^2 t/\tau_{ii}} \right], \quad (26)$$

where  $\Gamma = 0.585\epsilon^{1/2} + 0.529\epsilon$  and the ion-ion collision time  $\tau_{ii} = m_i^{1/2} (2T_i)^{3/2} / 4\pi e^4 n_0 \ln \Lambda$ . This analytical result has been compared to GS2 numerical simulations, as shown in Fig. 4. If momentum conservation in like particle collisions is not retained then the damping time changes from approximately  $\tau_{ii}\Theta/\Gamma \cong 2.7\epsilon\tau_{ii}$  to  $4\epsilon^{3/2}\tau_{ii}$ , and the agreement can be seen to be rather poor. For small  $\epsilon$ , such as  $\epsilon=0.1$ , our analytical result captures the main feature of the decay curve from the GS2 simulation. As  $\epsilon$  becomes larger ( $\epsilon=0.2$ ), our analytical result becomes less accurate since it assumes  $\epsilon \ll 1$ . Because the analytical formula is based on a multipole decay model that only retains a single collisional pole, it can only capture the main feature of the collisional decay,<sup>10</sup> and is unable to recover the very early time and long-time features of the damping process, as shown in Fig. 4. Even so, the consis-

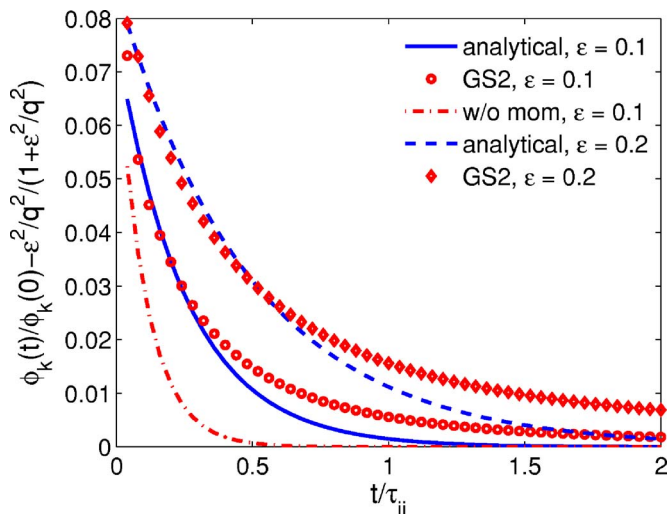


FIG. 4. Comparison between the analytical formula (continuous curves) and GS2 simulations (discrete shapes) of the collisional residual zonal flow damping for  $\epsilon=0.1$  and  $0.2$ . The solid and dashed curves are taken from Eq. (26). The dash-dotted curve is for  $\epsilon=0.1$  and retains pitch angle scattering with full energy dependence (Ref. 10), but without momentum conservation for ion-ion collisions.

tency with the GS2 simulations shows that this simple analytical formula (that gives a decay time about twice that of H-R) can be readily applied to benchmark other numerical codes.

## VII. DISCUSSION AND CONCLUSION

This paper provides a systematic review of the R-H collisionless and H-R collisional zonal flow damping and their recent extensions in three different directions. These three important extensions have been carefully tested by GS2 simulation. First, in the collisionless regime, the analytic scaling of shaping effects due to elongation and triangularity have been confirmed by GS2 simulation. Elongation, or the increase of poloidal field, is seen to substantially increase the zonal flow residual and may have important consequences in regulating turbulence. Next, short wavelength effects on the zonal flow residual as evaluated analytically and by GS2 simulation were found to be in agreement to remarkable accuracy. The increase of zonal flow residual for short wave-

lengths may indicate there is a strong impact on ETG turbulence when secondary instabilities produce the same amount of zonal flow as the ITG and TEM modes.<sup>24</sup> Finally, we investigated the collisional damping of zonal flow by comparing the GS2 simulation and the analytical result from a new eigenfunction expansion approach that improves on the H-R result. Quite good agreement is obtained in the large aspect ratio limit with a relatively simple approximation to the collisional response provided momentum conservation in like particle collisions is retained.

## ACKNOWLEDGMENT

This work was supported by U.S. Department of Energy Grant No. DE-FG02-91ER-54109 at the Massachusetts Institute of Technology and by the Center for Multiscale Plasma Dynamics.

- <sup>1</sup>W. Dorland and G. Hammett, *Phys. Fluids B* **5**, 812 (1993).
- <sup>2</sup>Z. Lin, T. Hahn, W. Lee, W. Tang, and R. White, *Science* **281**, 1835 (1998).
- <sup>3</sup>J. Candy and R. Waltz, *Phys. Rev. Lett.* **91**, 045001 (2003).
- <sup>4</sup>D. R. Ernst, P. T. Bonoli, and P. J. Catto, *Phys. Plasmas* **11**, 2637 (2004).
- <sup>5</sup>B. Coppi and G. Rewoldt, *Phys. Rev. Lett.* **33**, 1329 (1974).
- <sup>6</sup>M. Rosenbluth and F. Hinton, *Phys. Rev. Lett.* **80**, 724 (1998).
- <sup>7</sup>F. Hinton and M. Rosenbluth, *Plasma Phys. Controlled Fusion* **41**, A653 (1999).
- <sup>8</sup>Y. Xiao and P. Catto, *Phys. Plasmas* **13**, 082307 (2006).
- <sup>9</sup>Y. Xiao and P. Catto, *Phys. Plasmas* **13**, 102311 (2006).
- <sup>10</sup>Y. Xiao, P. Catto, and K. Molvig, *Phys. Plasmas* **14**, 032302 (2007).
- <sup>11</sup>W. Dorland, F. Jenko, M. Kotschenreuther, and B. Rogers, *Phys. Rev. Lett.* **85**, 5579 (2000).
- <sup>12</sup>Y. Lee, J. Dong, P. Guzdar, and C. Liu, *Phys. Fluids* **30**, 1331 (1987).
- <sup>13</sup>M. Kotschenreuther, G. Rewoldt, and W. Tang, *Comput. Phys. Commun.* **88**, 128 (1991).
- <sup>14</sup>A. M. Dimits, G. Bateman, and M. A. Beer, *Phys. Plasmas* **7**, 969 (2000).
- <sup>15</sup>F. Jenko, W. Dorland, M. Kotschenreuther, and B. Rogers, *Phys. Plasmas* **7**, 1904 (2000).
- <sup>16</sup>E. Belli, Ph.D. dissertation, Princeton University, 2006.
- <sup>17</sup>P. Catto, W. Tang, and D. Baldwin, *Plasma Phys.* **23**, 639 (1981).
- <sup>18</sup>P. Catto and K. Tsang, *Phys. Fluids* **20**, 396 (1977).
- <sup>19</sup>R. Miller, M. Chu, J. Greene, Y. Lin-Liu, and R. Waltz, *Phys. Plasmas* **5**, 973 (1998).
- <sup>20</sup>S. Zheng, A. Wootton, and E. Solano, *Phys. Plasmas* **3**, 1176 (1996).
- <sup>21</sup>G. R. McKee, F. J. Fonck, and M. Jakubowski, *Phys. Plasmas* **10**, 1712 (2003).
- <sup>22</sup>T. L. Rhodes, J.-N. Leboeuf, and R. D. Sydora, *Phys. Plasmas* **9**, 2141 (2002).
- <sup>23</sup>R. Waltz (private communication).
- <sup>24</sup>R. E. Waltz, J. Candy, and M. Fahey, *Phys. Plasmas* **14**, 056116 (2007).
- <sup>25</sup>E. Kim, C. Holland, and P. Diamond, *Phys. Rev. Lett.* **91**, 075003 (2003).